DOI 10.24425/aee.2023.145424

Non-linear effects of operation temperature on a field-coupled current-controlled inductance

GUIDO SCHIERLE ✉, MICHAEL MEISSNER, KLAUS F. HOFFMANN

Helmut Schmidt University
Germany
e-mail: ✉*guido.schierle@hsu-hh.de*

(Received: 14.09.2022, revised: 01.03.2023)

Abstract: In this publication the effect of the operating temperature on the effective inductance of a controllable inductor is analysed. The main difference compared to a coil with a simple single core lies in the current-controlled inductance-value. This is achieved by a second core implemented perpendicular upon the load-toroid affecting the saturation within a limited shared volume. Corresponding to the presented analysis, the dependencies on the core temperatures are investigated by measurements.

Key words: magnetic coupling, magnetic device, passive component

1. Introduction

Inductors have been widely used for lots of different purposes. Energy storage for buck- or boost-converters, inductive resonant tank elements for different types of resonant converters and inductors for filters could be mentioned as typical examples. Often, fixed optimal values can be found and corresponding devices can be implemented. In some applications, the availability of wide ranges of input or output parameters and a possibility to change on the fly would be desirable. This results almost always in a suboptimal compromise, because effects like saturation and losses have to be taken into account. Especially in suction circuits for filtering or resonant tank applications with changing parameters adaptable inductors may be a promising alternative. In particular, within the well-known quasi-resonant applications of the Auxiliary Resonant Commutated Pole Inverter (ARCPI) the resonant elements and thus the characteristic impedance have fixed values [1–4]. By the suggested adjustment of the resonant inductor the disadvantages of the ARCPI could be avoided by the adaption of the resonant current to the corresponding operation point.

Adjustable inductors and magnetic amplifiers as a part of them have been well-known for decades [5, 6]. Based on this knowledge different concepts for the usage of transducers and adjustable inductors have been developed and investigated in the past [7–9]. Nevertheless, it is not a research field with diminishing interest [10, 11].

For this reason and apart from other concepts an alternative setup consisting of two intersecting toroid cores with a control- and a load-winding is presented. This is depicted in Fig. 1.

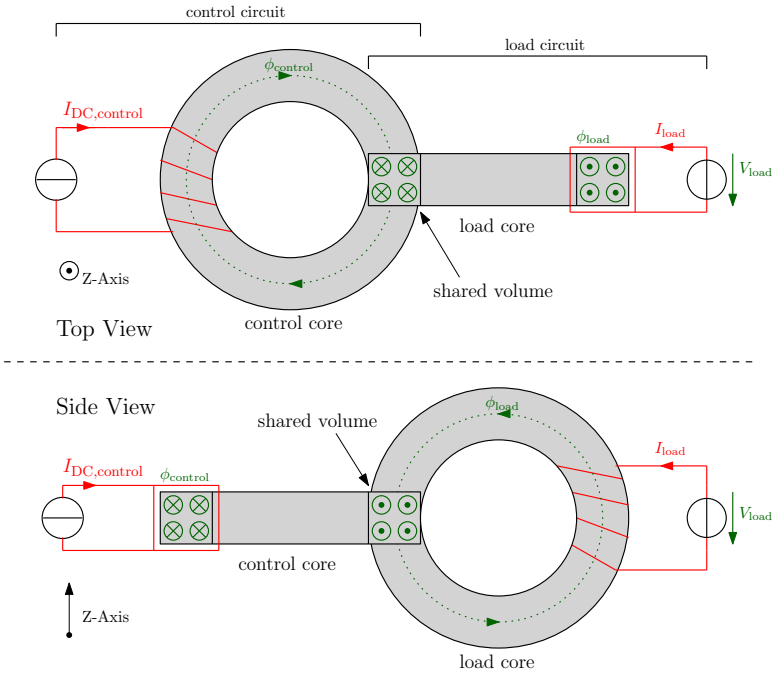

Fig. 1. Setup of the two intersecting toroid-cores, taken from [12]

Magnetic materials are known for a temperature dependence with the most significant effect of losing all properties at the Curie temperature. The relation between magnetic field strength and flux density changes already before, resulting in a distortion of the original *B*–*H*-curve. In this paper the focus of the presented investigations is on the dependence of the characteristic of the proposed setup on the operating temperature. This also includes the usability of this construction in corresponding applications.

In order to describe the temperature dependency, the setup has been implemented within a climate chamber and measured at three different ambient temperatures, which are –20°C, 25°C and 100°C, giving a maximal temperature interval of 120 K. At each temperature a series of measurements was conducted giving a set of curves characterizing the setup. The change of these curves indicates the temperature dependency. Control currents up to 30 A were applied, using the E-6 series, which gives corresponding logarithmic steps (often used for resistor values). The motivation for this was the assumption of a non-linear behavior of both the investigated effective inductance and the *B*–*H* characteristics.

For the chosen temperature of 100°C the stated saturation flux density drops significantly and the *B*–*H* characteristic flattens noticeable, which is observable in [12]. The transition to a fully saturated core material is reached with a lower magnetic field strength and more sudden. Additionally, this analysis could present interesting results, because 100°C is not an unusual operating temperature.

On the contrary, there are no information given about the behavior of the flux density for a temperature below 25°C. Again, the examination of the chosen minimal value of –20°C will display further insights into the characteristics of the presented setup. It will be interesting to see if there are any advantages which could prevail the need of cooling the system down. Both conditions will be investigated by measurements and presented in the following chapters.

2. Operation principle

As described, the setup consists of two intersecting toroid-cores with one winding each. The control winding is used to pre-magnetize the intersecting volume and therefore affect the inductance of the load winding. The realized setup can be seen in Fig. 2. In this analysis, both cores are made of the same magnetic material and are glued in the area of the shared volume. This is to ensure that there are no distortions for the different measurements resulting from possible changes in the size of the shared volume.

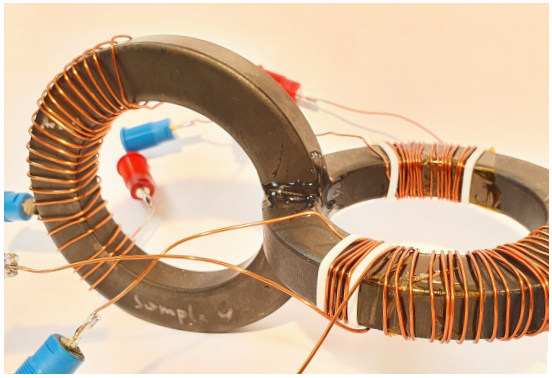

Fig. 2. Realized setup of the field-coupled current-controlled inductance

For investigation a ferrite from the company TDK, made of the material N30, with a number of turns of 5 for the winding of the load core and a number of turns of 22 for the winding of the control core was used [13]. Figure 3 shows the effect of the control current on the effective inductance and Fig. 4 shows the effect on the *B*–*H* characteristics at 25°C.

It can be seen that the effective inductance decreases with rising control current. Furthermore, the characteristic curve starts to flatten, which is expectable considering the shared volume of both cores as a variable air gap.

A general proof of concept is already given in [14] and is advanced with this publication by the investigation of the influence of the operating temperature to detect further possible degrees of

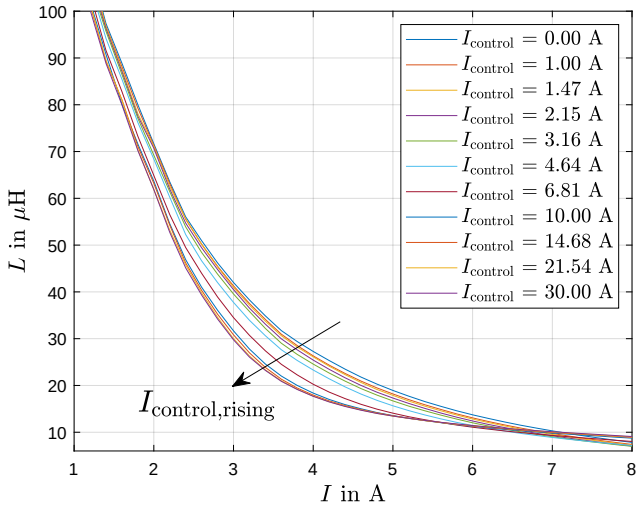

Fig. 3. Dependency of effective inductance on control current at 25°C and load current I

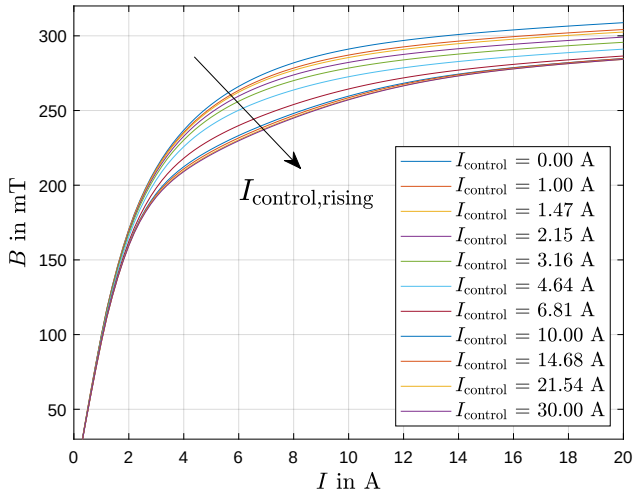

Fig. 4. Exemplary impact of control current on B–H characteristics at 25°C and load current I

freedom. The analysis of possible effects of the temperature run-up will allow conclusions about the characteristics of the presented setup right after switching it on and after a certain operation time. Additionally, it is well known that especially the high dependency of the effective inductance on the load current, observable in Fig. 3, and the low current load capacity are challenges, which need to be addressed in subsequent investigations on this promising concept.

3. Measurement method

For measurement, a system called Power Choke Tester DPG 20 was used, which applies a pulsed measurement method. For this, an internal capacitor bank is charged. Afterwards, the resulting square wave DC voltage is imposed on the DUT. According to the applied voltage, the current in the inductive load circuit starts to rise. The slew rate is dependent on the inductance L.As soon as a predefined maximum current is reached, the system stops the measurement. Since the device has a maximum of 100 sampling points, the inductance is calculated using the simplified Eq. (1). Additional information to the mode of operation can be found in [15].

$$v_L(t) = L(i) \cdot \frac{\Delta i(t)}{\Delta t} \,. \tag{1}$$

The magnetic flux density was also determined by this Choke Tester. The product of the inductance, derived by Eq. (1) and the current gives the flux linkage Ψ as Eq. (2) clarifies. The flux linkage is the product of the number of turns N and the magnetic flux Φ.

$$\Psi(i) = L(i) \cdot i = N \cdot \Phi. \tag{2}$$

Considering the magnetic cross section A_e, the magnetic flux density is calculated by the use of Eq. (3)

$$B(i) = \frac{\Psi(i)}{A_e \cdot N} \,. \tag{3}$$

The calculations based on the results of the measurement and used to determine the presented values are accurate enough to state general derivations of the influence of the operating temperature.

4. Measurement results

In this section the results of the measurements are presented. For reasons of clarity the description of the outcomes is divided into effects on effective inductance and effects on magnetic flux density due to the change of temperature. The measurement system was configured to stop the measurement once the load current reached 20 A. It was noticed that the load core was almost entirely saturated for all temperatures for this current.

4.1. Impact of temperature on effective inductance

In addition to the influence of control current on the effective inductance a change in operating temperature provides a further degree of freedom to have an impact on the inductor or another parameter to consider at usage. For this reason, the measurement presented in Fig. 3 was extended for an operating temperature of –20°C and 100°C. The results are presented in Fig. 5.

It can be seen that with rising control current and additionally with rising temperature the effective inductance decreases. For each family of curves there is an area, where the measurements curves intersect. The operating temperature dominates towards the control current as the total value of the decrease of effective inductance is higher for an increase in temperature than an

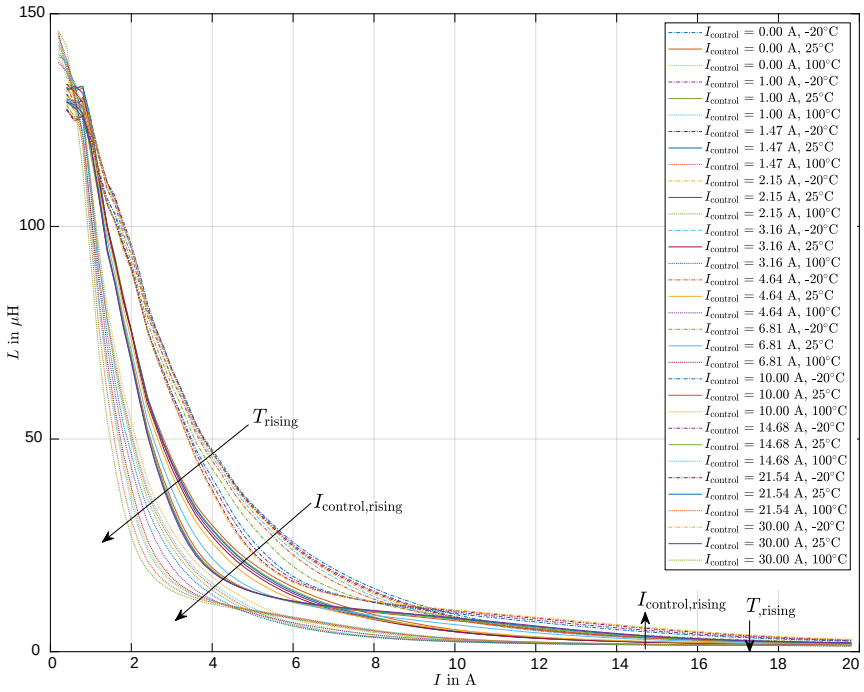

Fig. 5. Dependency of effective inductance on control current at different temperatures

increase in control current until the curves start to intersect. For example, at a load current of 2 A the effective inductance drops with the applied control current the most at an operating temperature of 100°C from around 60 µH to around 30 µH. A change of the temperature from –20°C to 100°C at the same load current decreases the inductance value from around 95 µH to around 60 µH without any control current applied. A more detailed investigation of the intersection behavior can be found in [14]. Contrary to this, a higher operation temperature still lowers the effective inductance.

For a more detailed presentation, the exemplary load-current values of 4 A and 12 A are enlarged and given in the Figs. 6 and 7.

At load currents of about 4 A both control variables decrease the effective inductance. The three temperature sets can be easily distinguished by the different line styles. Even though the first temperature step of 45 K is far less than the second of 75 K, the effects upon the effective inductance are decreasing, which outlines the high nonlinearity of the used material.

Contrary to the measurements at 4 A, the results at a load current of about 12 A (depicted in Fig. 7) show an increase of the effective inductance with rising control currents. This is the case at higher load currents at the right-hand side of the before mentioned intersection area. It should be noted that the scale is different to Fig. 6 so the differences in inductance are much smaller. For a temperature of 100°C the effect of the control current is almost neglectable.

The Figs. 8 and 9 are displays of the inductance versus the operating temperature including only three selected control current values. The before mentioned non-linearity in decrease of the

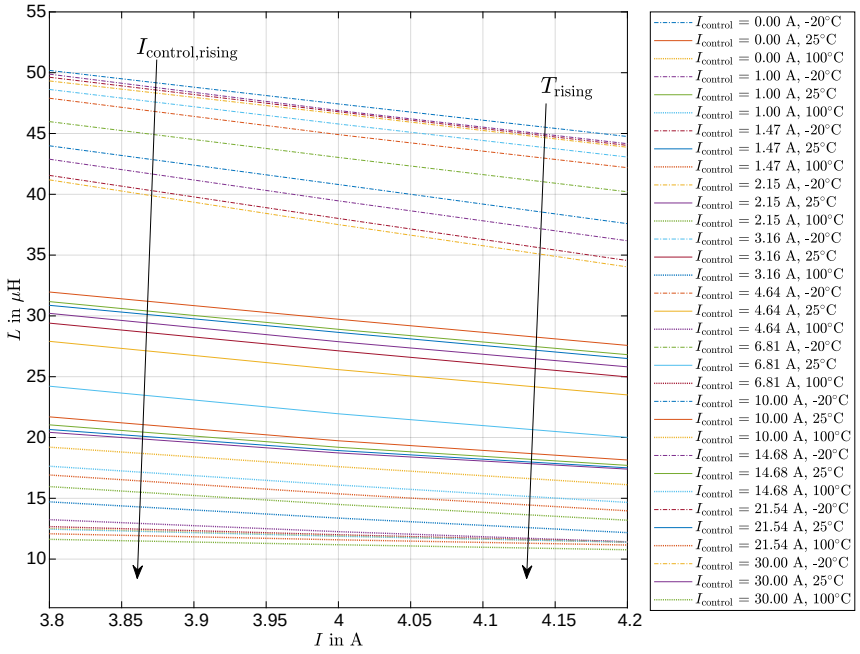

Fig. 6. Dependency of effective inductance on control current and temperature (enlarged)

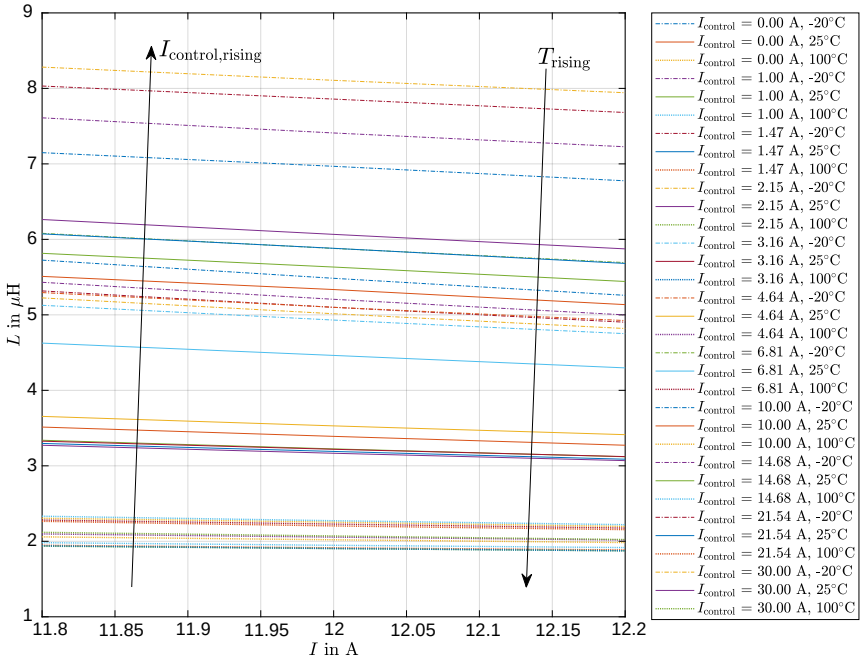

Fig. 7. Dependency of effective inductance on control current and temperature (enlarged)

effective inductance is clearly to see as all graphs with only one exception at high control and high load current show a steeper decent at lower temperatures.

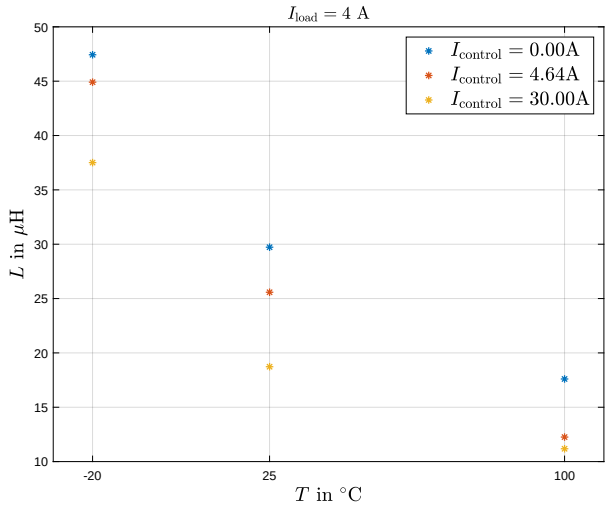

Fig. 8. Effective inductance vs. operating temperature for chosen control currents; $I_{\text{load}} = 4$ A

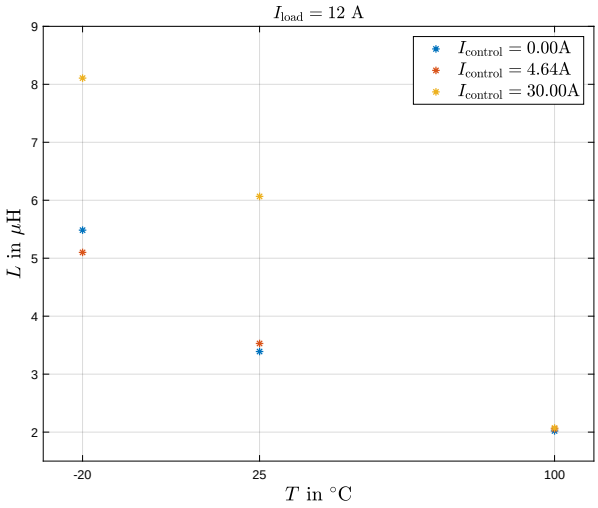

Fig. 9. Effective inductance vs. operating temperature for chosen control currents; $I_{\text{load}} = 12$ A

With higher load currents the effect of the control current is inverted as shown in [14]. Therefore, the absolute inductance value with a control current of 30 A exceeds the other. This also gives an interesting challenge or opportunity for control.

4.2. Impact of temperature on *B–H* characteristic

In order to show the basic effect on the *B–H* characteristic, the magnetic flux density is plotted against the load current. The magnetic field strength *H* could be used instead of the load current but only a proportionality factor would scale the following measurement curves.

According to the investigation of the effective inductance the measurement of the magnetic flux density, presented in Fig. 4, was extended by two operating temperatures of –20°C and 100°C and can be seen in Fig. 10.

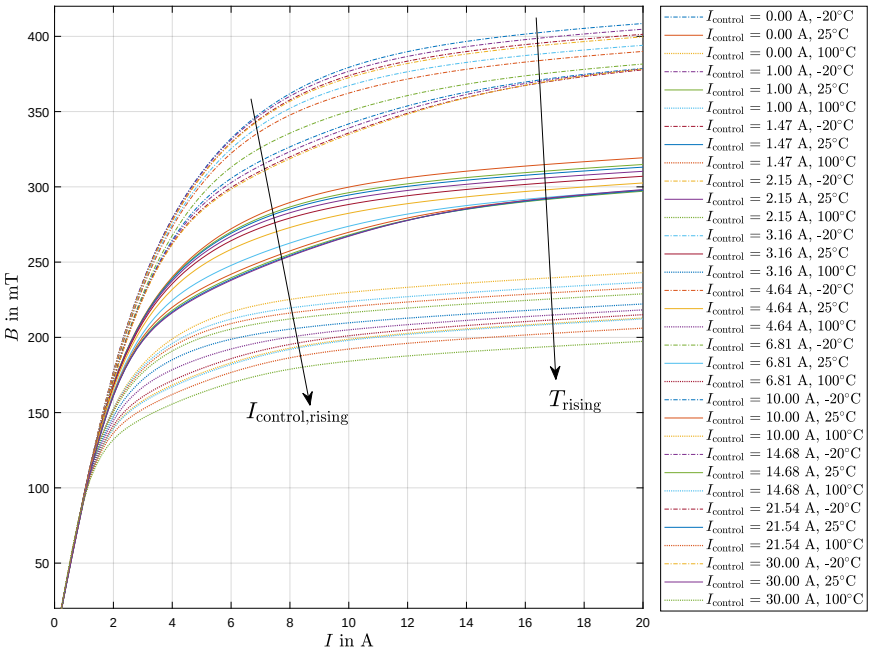

Fig. 10. Dependency of magnetic flux density on control current at different temperatures

It is clearly observable that the magnetic flux density decreases with increasing control currents. A rise of operating temperature enhances this effect. Moreover, the slope of the *B–H* characteristics lessens, meaning the saturation of the core material is reached at lower load currents. Proceeding from saturation at lower load currents, the effective inductance should drop for the same load current with rising operating temperatures. It is also presented, that for the chosen parameters (number of turns of the control winding, maximum of the applied control current and air gap within the control circuit) the influence of the operating temperature dominates. The results are consistent with the findings of the influence on effective inductance as a comparison with Fig. 5 illustrates.

For better visualisation, the exemplary load-current values of about 4 A and 12 A are enlarged once more and given in the Figs. 11 and 12. Furthermore, the influence of operating temperature and control current can be examined more closely.

Figure 11 clarifies the impact on the magnetic flux density. It is clearly observable that the slopes of the measurement curves decrease with higher temperatures and rising control currents. Taking a closer look, the influence of the temperature on the magnetic flux density compared to the control current seems to be stronger. While the control current only influences the slope marginally, the increase in temperature lowers the steepness significantly.

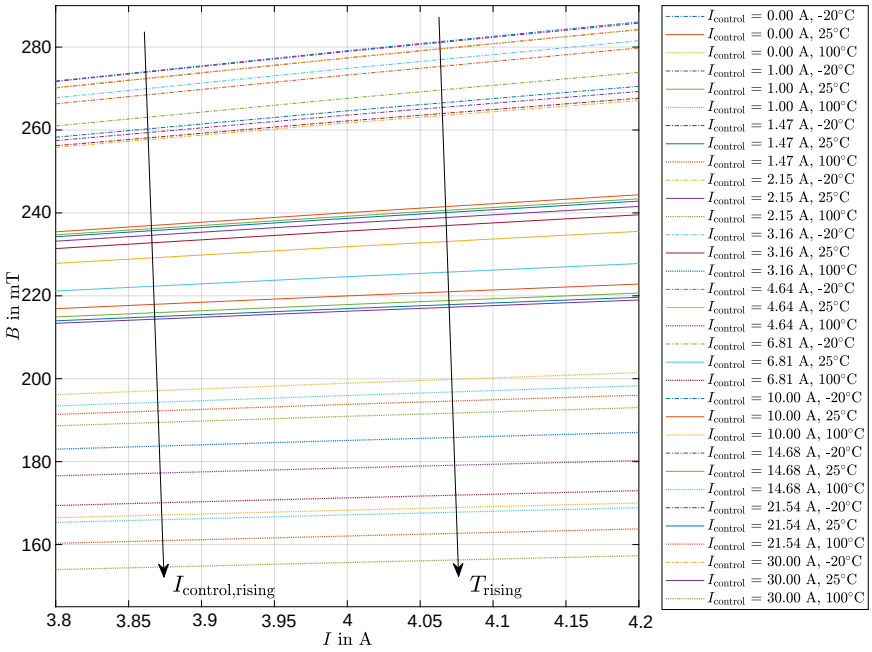

Fig. 11. Dependency of magnetic flux density on control current and temperature (enlarged)

An explanation of this behavior could be found in the characteristics of the used magnetic material and the proposed setup. A higher temperature influences the magnetic properties of the entire core by reducing the saturation flux density as the datasheet explains [13]. However, the control current has only an impact on the characteristics of a defined volume. Compared to the total volume of the core, the influence of the temperature dominates [16].

To outline the impact of the temperature Figs. 13 and 14 show the magnetic flux density vs. the operation temperature at a load current of about 4 A and 12 A, respectively. As for the investigation of the effective inductance three chosen values of control current are displayed.

For a load current of 4 A, the influence of the operating temperature is stronger than of the control current as Fig. 13 confirms. The drop of the magnetic flux density is significantly higher for increasing temperatures compared to the steps of the control current. Furthermore, it is recognizable that with a rise in operating temperature the influence of the control current is growing.

Figure 14 displays that the temperature still dominates the impact on inductance towards the control current.

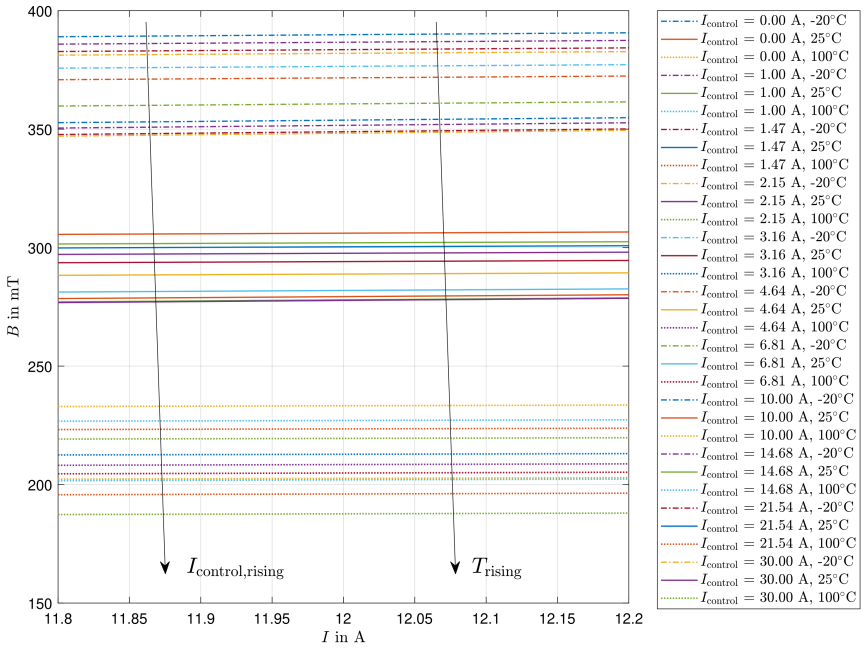

Fig. 12. Dependency of magnetic flux density on control current and temperature (enlarged)

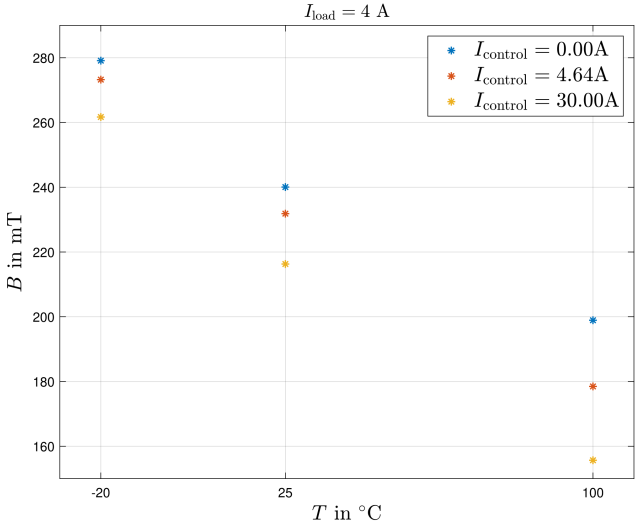

Fig. 13. Magnetic flux density vs. operating temperature for chosen control currents; $I_{\mathrm{load}} = 4$ A

Nevertheless, contrary to operation at lower load currents, a considerable increase in influence with rising control currents cannot be noticed. One reason could be that for this setup the magnetic material is in different states of saturation at the chosen temperatures.

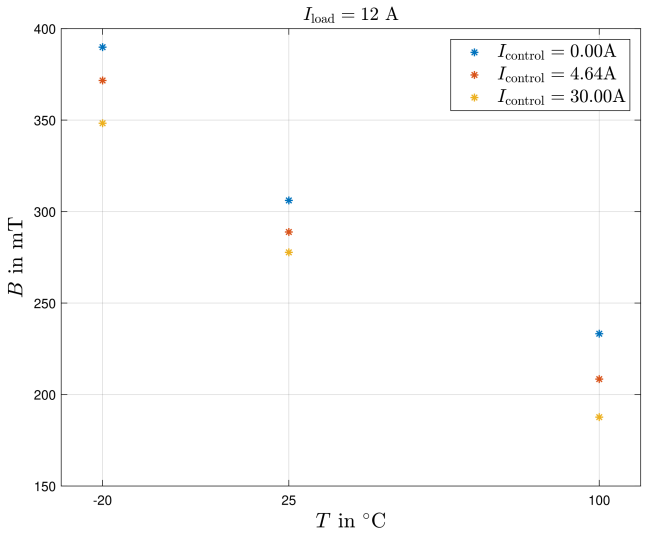

Fig. 14. Magnetic flux density vs. operating temperature for chosen control currents; $I_{\text{load}} = 12$ A

5. Conclusion

This paper presents the effects of operation temperature on a concept for an adjustable inductance. A decrease of the effective inductance at higher operating temperatures is clearly observable. The corresponding *B–H* characteristics flatten significantly with rising temperature. Comparing the impact of the control current and the temperature, latter one dominates the influence on the effective inductance clearly for the chosen parameters within this publication. The only detected exception could be found for the effective inductance at higher load currents.

Following from the remarkable dependency of the effective inductance on operating temperature, a noteworthy degree of freedom is described. For an implementation of this concept into an electric circuit, this presented dependency could lead to an interesting challenge or opportunity for control and should be taken into account.

In future investigations a realized setup consisting of cores made from different materials will be analysed in order to reduce the high dependency of the inductance on the load current. Moreover, the interaction between temperature, control current and saturation of the core material could be investigated more closely with a different set of parameters.

References

[1] Xiaoming Yuan, Orglmeister G., Barbi I., *ARCPI resonant snubber for the neutral-point-clamped inverter*, in IEEE Transactions on Industry Applications, vol. 36, no. 2, pp. 586–595 (2000), DOI: 10.1109/28.833777.

[2] Fujii K., Koellensperger P., De Doncker R.W., *Characterization and comparison of high blocking voltage IGBTs and IEGTs under hard- and soft-switching conditions*, 2006 37th IEEE Power Electronics Specialists Conference, Jeju, South Korea, pp. 1–7 (2006), DOI: 10.1109/pesc.2006.1712138.

[3] Ma D., Wang P., Wang R., Li S., Sun Q., *Hybrid SVPWM Modulation Strategy for Auxiliary Resonant Commutated Pole Inverter*, in IEEE Journal of Emerging and Selected Topics in Power Electronics, vol. 9, no. 4, pp. 4750–4761 (2021), DOI: 10.1109/JESTPE.2020.3031643.

[4] Wang Q., Li L., Wang Y., *An Improved Auxiliary Resonant Commutated Pole Inverter with Low Loss of Energy Recovery*, in IEEE Transactions on Circuits and Systems II: Express Briefs, vol. 70, no. 2, pp. 655–659 (2023), DOI: 10.1109/TCSII.2022.3207945.

[5] Kümmel F., *Regel-Transduktoren. Theorie und Anwendungen in der Regelungstechnik*, Springer (1961).

[6] Tez E.S., *The Parametric Transformer*, PhD Thesis, Loughborough University of Technology (1977).

[7] Kaerst J.P., Hoffmann K., *Transductor based high speed gate drive*, 2004 IEEE 35th Annual Power Electronics Specialists Conference (IEEE Cat. No. 04CH37551), vol. 1, pp. 100–104 (2004), DOI: 10.1109/PESC.2004.1355722.

[8] Kaerst J.P., Hoffmann K., *Design Rules for Transductor based Gate Drives*, Power Conversion and Intelligent Motion Conference-PCIM (2005).

[9] Zacharias P., Kleeb T., Fenske F., Wende J., Pfeiffer, *Controlled magnetic devices in power electronic applications*, 2017 19th European Conference on Power Electronics and Applications (EPE'17 ECCE Europe), pp. P.1–P.10 (2017), DOI: 10.23919/EPE17ECCEEurope.2017.8099004.

[10] Saeed S., Garcia J., Perdigão M.S., Costa V.S., Baptista B., Mendes A.M.S., *Improved Inductance Calculation in Variable Power Inductors by Adjustment of the Reluctance Model Through Magnetic Path Analysis*, in IEEE Transactions on Industry Applications, vol. 57, no. 2, pp. 1572–1587 (2021), DOI: 10.1109/TIA.2020.3047593.

[11] Brandt S., Meissner M., Polap N., Schierle G., Hoffmann K.F., *A Survey on Adjustable Inductances for Power Electronic Circuits*, PCIM Europe 2022; International Exhibition and Conference for Power Electronics, Intelligent Motion, Renewable Energy and Energy Management, pp. 1–9 (2022), DOI: 10.30420/565822219.

[12] Magel D., *Implementation, Analysis and Comparison of Different Prototypes of Current Controlled Inductors for Power Electronic Applications*, Bachelor Thesis, Helmut Schmidt University (2022).

[13] TDK, *Siferrit material N30*, in Ferrites and accessories (2017).

[14] Schierle G., Meissner M., Hoffmann K.F., *Analysis and Discussion of a Concept for an Adjustable Inductance Based on an Impact of an Orthogonal Magnetic Field*, 2022 24th European Conference on Power Electronics and Applications (EPE'22 ECCE Europe), pp. 1–10 (2022).

[15] ed-k, *Power Choke Tester DPG10 B - Serie & DPG 20*, Manual (2020).

[16] TDK, *Toroids (ring cores) R 102 × 65.8 × 15.0*, in Ferrites and accessories (2017).